

High-pressure phase diagram, structural transitions, and persistent non-metallicity of BaBiO₃: theory and experiment

Roman Martoňák,¹ Davide Ceresoli,² Tomoko Kagayama,³ Yusuke Matsuda,³ Yuh Yamada,⁴ and Erio Tosatti^{5,6}

¹*Department of Experimental Physics, Comenius University, Mlynská Dolina F2, 842 48 Bratislava, Slovakia*

²*CNR Institute of Molecular Science and Technology (ISTM), via Golgi 19, 20133 Milan, Italy*

³*KYOKUGEN, Graduate School of Engineering Science, Osaka University,*

Machikaneyamacho 1-3, Toyonaka, Osaka 560-8531, Japan

⁴*Department of Physics, Faculty of Science, Niigata University,*

8050, Ikarashi 2-no-cho, Nishi-ku, Niigata 950-2181, Japan

⁵*International School for Advanced Studies (SISSA) and CNR-IOM Democritos, Via Bonomea 265, I-34136 Trieste, Italy*

⁶*The Abdus Salam International Centre for Theoretical Physics (ICTP), Strada Costiera 11, I-34151 Trieste, Italy*

(Dated: October 4, 2018)

BaBiO₃ is a mixed-valence perovskite which escapes the metallic state through a Bi valence (and Bi-O bond) disproportionation or CDW distortion, resulting in a semiconductor with a gap of 0.8 eV at zero pressure. The evolution of structural and electronic properties at high pressure is, however, largely unknown. Pressure, one might have hoped, could reduce the disproportionation, making the two Bi ions equivalent and bringing the system closer to metallicity or even to superconductivity, such as is attained at ambient pressure upon metal doping. We address the high-pressure phase diagram of pristine BaBiO₃ by ab initio DFT calculations based on GGA and hybrid functionals in combination with crystal structure prediction methods based on evolutionary algorithms, molecular dynamics and metadynamics. The calculated phase diagram from 0 to 50 GPa indicates that pristine BaBiO₃ resists metallization under pressure, undergoing instead at room temperature structural phase transitions from monoclinic *I2/m* to nearly tetragonal *P-1* at 7 GPa, possibly to monoclinic *C2/m* at 27 GPa, and to triclinic *P1* at 43 GPa. Remarkably, all these phases sustain and in fact increase the inequivalence of two Bi neighboring sites and of their Bi-O bonds and, in all cases except semimetallic *C2/m*, the associated insulating character. We then present high-pressure resistivity data which generally corroborate these results, and show that the insulating character persists at least up to 80 GPa, suggesting that the *C2/m* phase is probably an artifact of the small computational cell.

I. INTRODUCTION

BaBiO₃ is a narrow gap insulating perovskite of considerable importance on several accounts. The first is that the insulating state is accompanied, and in fact caused, by a relatively small displacive structural dimerizing CDW-like lattice distortion,¹ also amounting to a spontaneous static mixed valence disproportionation of two otherwise equivalent Bi cations from nominal valency 4+ to 3+/5+² (see also Fig.1 in Ref.³). Another is that the insulating and distorted state reverts to an undistorted metal upon hole doping in alloys such as Ba_{1-x}K_xBiO₃ yielding an important class of superconductors, with T_c as high as 30 K^{4,5}. Superconductivity in these systems has been discussed as a classic example of what came to be called a bipolaron state, whereby quantum fluctuations turn the static electron pairing around the fixed Bi(3+) ion sublattice into a dynamical state. The quantum mechanically delocalized electron pairs can then make all Bi sites dynamically equivalent in the superconducting state².

The structural behaviour of BaBiO₃ is non-trivial already at zero pressure where it undergoes three phase transitions with temperature. The low temperature structure with space group *P2₁/n* was first resolved by Kennedy et al.⁶ by neutron diffraction and is stable below 132 K, where it transforms to the *I2/m* structure

which is the room temperature form studied by Cox and Sleight¹. This form is stable until 430 K where it further transforms into a rhombohedral *R-3* structure. Finally at 820 K BaBiO₃ transforms to a cubic structure with space group *Fm-3m*. The bond disproportionation persists all along these phases. The main difference between them consists of different rotation patterns of the BiO₆ octahedra⁶, rotations which must therefore involve small energy scales of the order of the thermal energy ~ 0.01 eV. Moreover, external perturbations including e.g., friction and strain could easily provoke transitions between them. For a recent review of structural and electronic aspects see Ref.⁷.

BaBiO₃ has been the subject of numerous theoretical studies,^{3,5,8,9} initially underlining the difficulty to reproduce within standard density functional theory (DFT) the dimerized insulating state at zero pressure, instead of an undimerized metal. Subsequent work showed that the problem is to some extent cured by appropriate choices of the exchange-correlation potential¹⁰ or by LDA+U underlining the delicate role of correlations in the zero-pressure state.^{11,12} None of that work, however, considered a prediction of the high-pressure phase diagram until the recent unpublished work of Smolyanyuk et al¹³ which does not contain experimental data but with whose theoretical results we make good reciprocal contact.

Experimentally, Akhtar et al¹⁴ provided an equation of state of pristine BaBiO₃ up to 10 GPa. Sugiura and

Yamadaya¹⁵ went up to 20 GPa and found X-ray diffraction and Raman evidence of a structural transition at 8-10 GPa to an unidentified tetragonal phase. Other work^{16,17} suggested a decrease of electronic gap for pressures up to 9 GPa, thus still within the initial $I2/m$ phase. What phase or phases will appear above 10 GPa, whether they would give up the disproportionation and metallize, or even superconduct, is still unknown.

We here explore these questions, both theoretically by ab initio calculations and experimentally by high-pressure resistivity measurements. Calculations including total-energy based evolutionary structure search¹⁸ as well as molecular dynamics and metadynamics¹⁹⁻²¹ simulations, indicate at room temperature a first structural phase transition from $I2/m$ to a nearly tetragonal $P-1$ symmetry around 7 GPa, whose surprising offshoot is that disproportionation of the two Bi cations as well as insulating character are preserved and actually enhanced by pressure, rather than eliminated. Upon further increase of pressure two rather unusual structures with space groups $C2/m$ and $P1$ are found, both of them disproportionated even if only the second frankly insulating. Experimental resistivity although unable to address the structure, shows near 10 GPa a phase transition from an insulating phase to another, with no metallic phases and a gap increasing at least until 40 GPa when the gap levels off.

The paper is organized as follows. In Section II we provide some details about the computational methodology used. In Section III we describe the experimental measurement of resistivity at high pressure. In Section IV we show the results of our evolutionary structural search and MD and metadynamics simulations, discuss the structural and electronic properties of the new phases and compare to experimental data. In Section V we draw our conclusions.

II. COMPUTATIONAL METHODS

Crystal structure prediction in this system represents a computational challenge. One reason is the difficulty of standard LDA or GGA functionals to properly describe the energetics of the system.^{3,5,8,9} While this appears to be cured by using the hybrid functional,¹⁰ it is not easy to perform evolutionary search using the latter because of its high computational cost. Moreover, the fact that already at $p = 0$ the system between zero and room temperature undergoes a temperature-induced structural transition points to the importance of entropic effects, neglected in standard prediction schemes based on e.g. evolutionary algorithms. For this reason we complement our study with molecular dynamics simulations, where entropy is included. In order to study structural transformations including kinetic effects we also apply the metadynamics¹⁹-based approach to structural phase transitions simulation^{20,21} which is able to cross barriers and dynamically follow structural transformations.

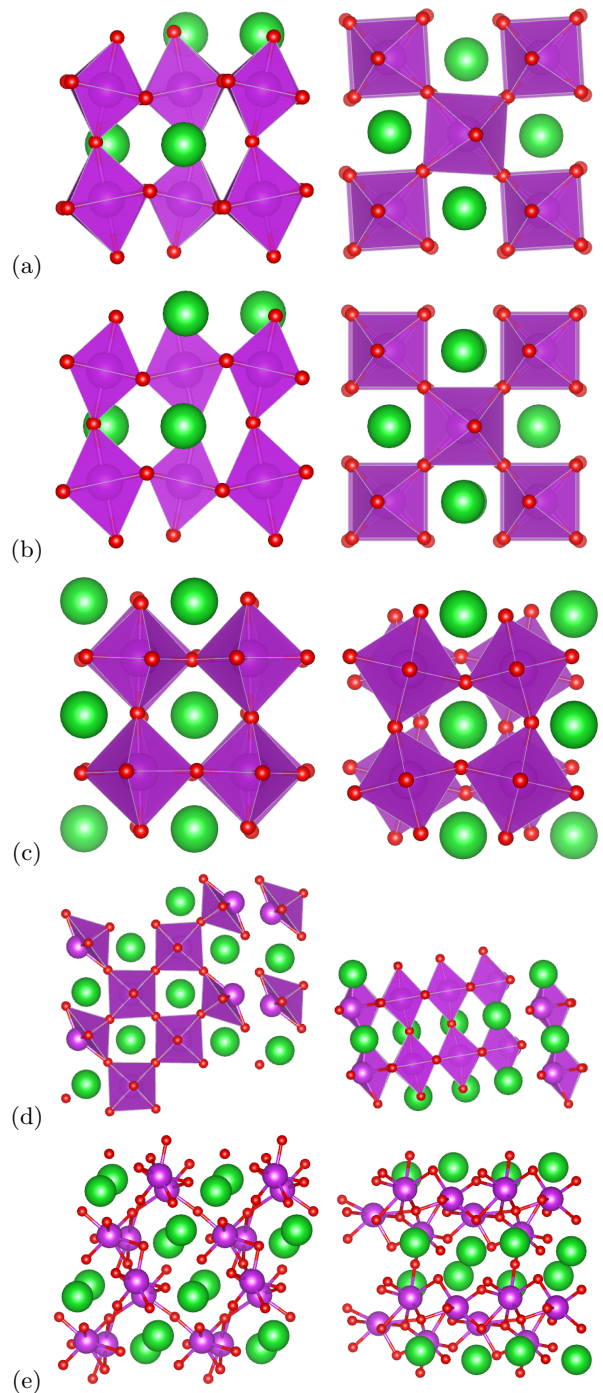


FIG. 1: $P2_1/n$ at 0 GPa (a), $I2/m$ at 0 GPa (b), $P-1$ at 20 GPa (c), $C2/m$ at 30 GPa (d) and $P1$ (e) at 50 GPa, respectively. Note that $C2/m$ can be obtained from ideal perovskite by creating a stacking fault and $P1$ is disordered.

We performed the evolutionary crystal structure search by using the Xtalopt code²² in combination with the VASP package^{23,24}. All calculations employed PAW pseudopotentials with 10 valence electrons ($5s^25p^66s^2$) for Ba, 15 electrons ($5d^{10}6s^26p^3$) for Bi and 6 electrons ($2s^22p^4$) for O. During the search the exchange-

correlation energy was calculated within the PBE²⁵ functional and an energy cutoff of 520 eV. The structural optimization was performed in several steps using tighter convergence criteria and denser Monkhorst-Pack²⁶ grids in later steps. To begin with, below 10 GPa the stability and structure of both $P2_1/n$ and $I2/m$ phases were checked and optimized. The subsequent structural search was carried out at pressures of 20, 30 and 40 GPa with a supercell containing four formula units (20 atoms). At both 20 GPa and 30 GPa the search generated more than 2000 structures. At 40 GPa we first generated more than 1000 structures. Afterwards we selected eight best structures and doubled the cell in one direction, thus creating cells with 40 atoms. These eight structures were subsequently used as seeds for an additional search at the same pressure which generated more than 1500 structures. The 40 atom supercell search, however, yielded no better structure than the 20 atoms cell search. The zero temperature structural search results should therefore be considered reliable within the usual limitations of limited number of structures generated and limited number of atoms in unit cell.

The most favorable structures generated by the search were subsequently refined by high accuracy electronic structure calculations. Structures, enthalpies and band structures with careful determinations of band gaps were obtained by using the HSE06 hybrid functional^{27,28}, shown by Franchini et al.¹⁰ to correctly reproduce structural parameters, bond disproportionation and band gaps.

III. EXPERIMENTAL - HIGH PRESSURE RESISTIVITY

Single crystals of BaBiO_3 were grown by cooling a melt of polycrystalline specimen in an alumina crucible from 900 to 600 °C at a rate of 2 °C/h in a higher oxygen atmosphere. The pressure was generated by the diamond anvil cell technique with a pair of diamond anvils of 150 microns culet. A gasket was made by a holed (70 micron in diameter) rhenium sheet subsequently covered with a mixture of cubic-boron-nitride powder and epoxy resin on a surface which plays both roles of a pressure transmitting media and electrical insulator to electrodes. The electrical resistance was measured with an electrometer using two platinum foil strip electrodes.

The pressure was determined by a fluorescence method with a ruby chip mounted on the sample as a standard material. The pressure dependence of the resistivity in the interval from 0 to 80 GPa is shown in Fig.2.

The resistivity initially decreases, in agreement with earlier data by Imai¹⁷ and at 8 GPa reaches about 80% of the value at 5 GPa. Beyond 8 GPa it, however, starts to grow and the ratio of resistivity at 40 and 10 GPa is about 35 (Fig.2). Assuming a simple exponential dependence of resistivity on the gap these numbers at room temperature imply an initial decrease of the gap between

5 and 8 GPa by 6 meV followed by increase by 92 meV between 10 and 40 GPa. The latter increase corresponds to the slope of about 30 meV/10 GPa. A large hysteretic behaviour is clearly seen upon pressure decrease suggesting that pressurization induces a major change in the system, possibly a reconstructive transition resulting in a barrier preventing the high-pressure state from returning to the original state.

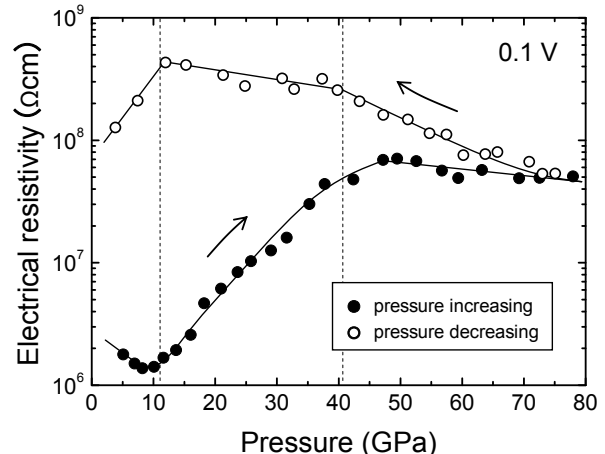


FIG. 2: Experimental data for resistivity of BaBiO_3 under pressure.

IV. THEORETICAL RESULTS

The structural search performed at pressures of 20, 30 and 40 GPa provided several new low enthalpy structures, nearly monoclinic $C2/c$ and nearly tetragonal $P-1$, monoclinic $C2/m$ and triclinic $P1$. In order to determine the phase stability at finite temperature one should compare the Gibbs free energies of the respective phases. An accurate calculation of free energies in this case is, however, difficult, for the reasons mentioned in Sec.II, especially at low pressures where the PBE functional might not be reliable, and the room temperature entropic effects are larger. We therefore limit ourselves to comparison of enthalpies shown in Fig.3 and we will comment about possible thermal effects where appropriate.

A. Crystal structure

1. Pseudotetragonal $P-1$ phase

Evolutionary search at 20 GPa provided several structures with low $P-1$ symmetry and very close enthalpies. Structurally they are still related to disproportionated perovskite and differ by very tiny distortions of the octahedra. The lowest enthalpy structure among them is close to monoclinic symmetry $C2/c$ followed by several

structures with enthalpy higher only by up to 2.3 meV per f.u. (0.46 meV per atom) which are very close to tetragonal symmetry and within a tolerance of 0.06 Å can be identified with space group $I4/m$. These minute enthalpy differences are not likely to survive at room temperature where they are likely to be washed out by thermal fluctuations. The common feature of all these structures is that they represent small variations of tetragonal perovskite structure similar to what SrTiO_3 adopts below 110 K²⁹ where octahedra are rotated around z -axis in an antiferrodistortive manner (space group $I4/mcm$) – the additional feature here being the bond disproportionation. Since in Ref.¹⁵ a transition to a tetragonal structure was reported between 8-10 GPa we consider the pseudotetragonal P -1 structures (see Fig.1) more representative of the room temperature structure above 10 GPa. Therefore we limited ourselves to pick one of these structures and use it in subsequent calculations³¹.

According to the enthalpy plot (Fig.3) the P -1 phase replaces the $P2_1/n$ phase at $p = 7$ GPa – note that P -1 has a slightly smaller volume (by 0.2 % at 10 GPa) compared to the $P2_1/n$ phase. The disproportionation pattern of Bi-O bonds in P -1 is identical to that of the low-pressure $P2_1/n$ and $I2/m$ structures where expanded and collapsed octahedra are arranged in an fcc-like arrangement (similar to rocksalt). The octahedra are rotated with respect to the ideal perovskite structure around the z axis, by an average rotation angle of 13.15° . (Fig.1).

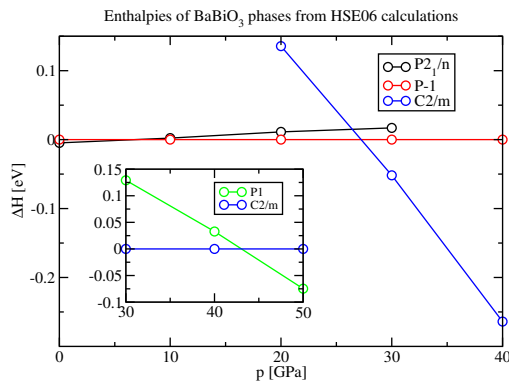


FIG. 3: Enthalpies (per formula unit) of various BaBiO_3 phases as function of pressure. In the main figure enthalpies are relative to the P -1 phase and the inset shows the enthalpy of the P 1 phase relative to the $C2/m$ phase.

Our predicted pseudotetragonal P -1 phase can be favorably compared to the available experimental data for the lattice parameters of the unidentified tetragonal structure discovered by Sugiura and Yamadaya¹⁵ at 8-10 GPa. In Fig.4 we show the pressure dependence of pseudotetragonal lattice parameters a, c of our zero-temperature P -1 phase. With increasing pressure the c/a ratio increases deviating further from 1, a feature which qualitatively agrees with the experimental data in

Ref.¹⁵, Fig.1.

Since the zero temperature $P2_1/n$ phase is replaced by $I2/m$ at room temperature, it is possible that P -1 might also undergo some kind of transition between zero and room temperature. In order to assess the importance of thermal effects we carried out an ab-initio variable-cell NPT molecular dynamics (MD) simulation at $p = 20$ GPa and $T = 300$ K employing a Parrinello-Rahman barostat³⁰ and a Langevin thermostat. The MD simulation was started from the ideal perovskite structure in cubic $2 \times 2 \times 2$ supercell (40 atoms) and dynamically simulated for 15000 steps representing a 30 ps time interval. Since the barriers between structures differing by octahedra rotation pattern in such small system are likely to be small the procedure may be expected to provide a realistic result for the room temperature structure.

The time evolution of cell parameters from this run is shown in Fig.5. It is seen that the lengths of the 3 supercell edges a, b, c , initially equal in the ideal perovskite structure, quickly split, into one longer and 2 shorter cell edges, the latter two equal on average. This transformation is related to the rotation of octahedra which takes place precisely in tetragonal SrTiO_3 -like manner, similar to the pseudotetragonal P -1 structure. This gives high confidence that the SrTiO_3 -like octahedra rotation pattern is a robust feature and the structure observed in the MD run indeed represents the stable minimum of the Gibbs free energy at room temperature and $p = 20$ GPa. While a much longer run would be necessary to accurately determine average values of the cell lengths and angles, the latter are seen to fluctuate around 90 degrees, a fact which together with the splitting of the cell lengths suggests that the P -1 structure appears tetragonal at room temperature (note that the tetragonal axis switches among various directions during the run because of the small size of the system). The c/a ratio from MD at 20 GPa is estimated to be about 1.025 which is smaller than the zero temperature value of 1.031 (Fig.4) and very close to the experimental value of 1.024 from Ref.¹⁵ (Fig.1).

In order to cross-check our prediction from the evolutionary algorithm we annealed the final structure from the NPT MD run at 300 K by lowering the temperature in 2 steps, first to 150 K and then to 30 K and performing at each temperature a 16 ps NPT MD run. The final structure from the 30 K run was structurally relaxed at $p = 20$ GPa and resulted again in a P -1 structure (very close to tetragonal $I4/m$) with enthalpy only 2.5 meV/f.u. above the best P -1 found at the same pressure by evolutionary search. This provides a strong independent confirmation of the validity of the evolutionary search.

In Fig.6 we show the pressure evolution of the bond disproportionation defined as difference between the average Bi-O bond length in expanded and collapsed octahedra, respectively. In both $I2/m$ and P -1 phases this imbalance is seen to slightly decrease with increasing pressure.

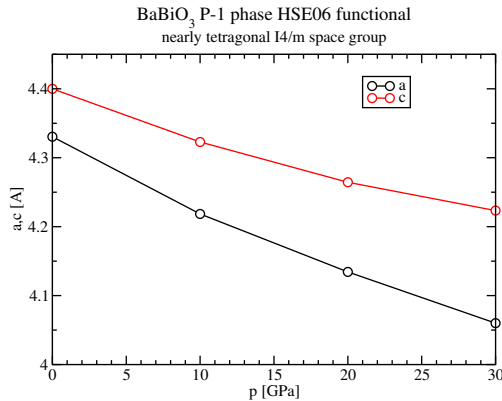


FIG. 4: Pressure dependence of the pseudotetragonal lattice parameters of P-1 structure.

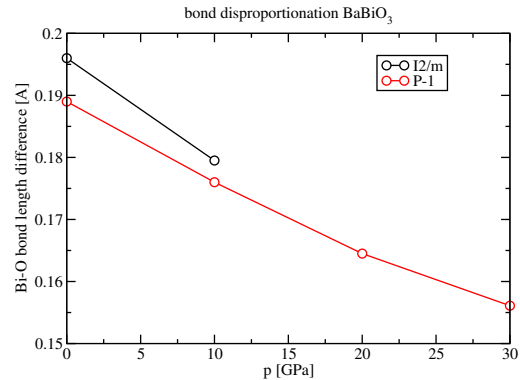


FIG. 6: Pressure dependence of the bond disproportionation in $I2/m$ and $P-1$ $BaBiO_3$.

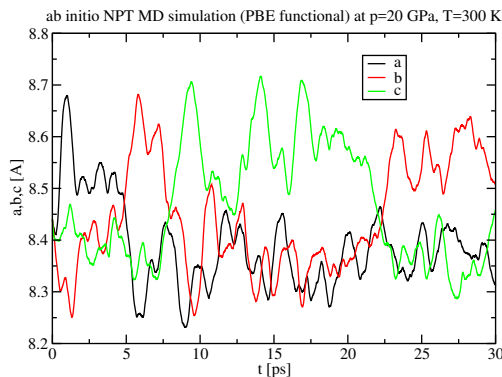


FIG. 5: Time evolution of supercell parameters during MD run at $p = 20$ GPa and $T = 300$ K.

2. Monoclinic $C2/m$ phase

A second structure was identified within our evolutionary search at 30 and 40 GPa which, with a space group $C2/m$, can be regarded as a perovskite structure with a stacking fault (Fig.1). Its volume at 30 GPa is 4.7 % lower than that of $P-1$ phase. This phase maintains two inequivalent Bi atoms in a rather unusual manner, by partly preserving and partly breaking the parent perovskite structure. This results in different local environments, one close to perovskite and the other not. Altogether, here we have a much stronger inequivalence of the two Bi ions than that realized at lower pressure by bond disproportionation. According to the enthalpy calculations it is stable from 27 GPa till 43 GPa (Fig.3).

3. Triclinic $P1$ phase

The next structure identified within the evolutionary search at 40 GPa has no symmetry and appears totally

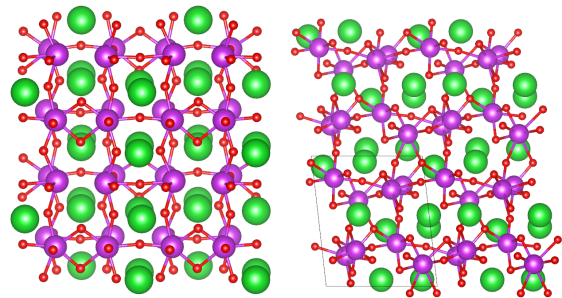


FIG. 7: Structures found by ab-initio metadynamics starting from the ideal perovskite at $T = 300$ K and $p = 50$ GPa. First defects are created (left panel) and finally a disordered structure is formed (right panel).

different from perovskite. Interestingly, it is nearly layered (Fig.1). There are still at least two inequivalent Bi ions, but there are no well defined coordination polyhedra around them. The volume of this $P1$ phase at 40 GPa is 1.4 % lower than that of $C2/m$ phase. According to the enthalpy calculations it is stable with respect to the $C2/m$ phase above 43 GPa (Fig.3).

Unlike the lower pressure $P-1$ slightly distorted perovskite, neither the $C2/m$ nor the $P1$ phases represent a small distortion of parent high-symmetry structure. For this reason they appear less likely to undergo a structural transformation between zero and room temperature due to entropic effects. We note that the structural disorder in $P1$ phase could also be related to a possible tendency to chemical decomposition at high pressure.

Altogether, both $C2/m$ and $P1$ structures appear somewhat dubious. They show either an unusual and composite atomic arrangement ($C2/m$) or disorder and no symmetries ($P1$), suggesting that they could be artifacts of the specific finite-size cell used in evolutionary search, especially if the true thermodynamically stable crystal structure might have a larger cell, possibly with higher symmetry (especially in the case of $P1$). The

true ground state might involve a complex arrangement of atoms only reachable in the search after many more generated structures. This question must be left for the future since extension of the present study in either direction is at the moment prohibitively demanding.

Experimentally, even if there were a complex thermodynamically stable structure with large unit cell, it might not be easy to reach for kinetic reasons in high-pressure experiment. It is therefore plausible that neither $C2/m$ and $P1$ are seen in experiment. Instead, $P-1$ or some similar form, still related to perovskite structure, might survive as metastable structure beyond 27 GPa until it reaches the limit of mechanical stability.

In order to investigate what might be happening at 50 GPa and beyond we applied the metadynamics¹⁹-based approach^{20,21}. The simulations were started from ideal perovskite structure on a supercell with 40 atoms and performed at $p = 50$ GPa and $T = 300$ K. Two typical structures from this simulation are shown in Fig.7 and represent a possible experimental outcome of pressurizing $P-1$. The structure on the left panel in Fig.7 represents a heavily distorted perovskite with a massive Bi disproportionation which further evolves towards disordered structure with tendency towards creation of layers (right panel in Fig.7), in fact similar to the predicted $P1$. The fact that these structures appear in metadynamics simulation shows that they are likely much easier to be reached kinetically rather than the search-predicted $C2/m$ and $P1$. We suspect that the structures observed in the resistivity experiment beyond 50 GPa might well be of this kind.

B. Electronic structure

As anticipated, in none of the phases theoretically predicted for high pressure BaBiO_3 all the Bi ions become equivalent. In line with that result, we expect that all these phases should be insulating, or nearly insulating. In order to check this important aspect we performed the electronic band structure calculation using the hybrid functional HSE06 – the method of choice which gave correct results at low pressures. Since both $I2/m$ and $P-1$ phases represent relatively small distortions of the ideal perovskite structure the Brillouin zone of both phases is similar to that of fcc phase (Fig.9, see also Fig.1 in Ref.⁸). We calculated the band structure of both phases and found it to be qualitatively similar to that found for artificially disproportionated ideal perovskite structure without octahedra rotation by Thonhauser and Rabe³. In their idealized case the indirect band gap in the LDA approximation opened up between the W and L points. In our case where we use the real energy-minimized HSE06 $I2/m$ structure, the highest occupied band between the W and X points is remarkably flat. This implies that the indirect band gap is likely to open between the valence band maximum (VBM) in the segment between W and X and conduction band minimum in L. Due to symmetry

breaking related to the rotation of octahedra, however, degeneracy of bands at special points in BZ in ideal cubic perovskite structure is lifted, as can be seen in Figs.8 and 9. In the $I2/m$ structure the VBM is at the point X while in the $P-1$ phase it is at the point Z on the pseudotetragonal axis.

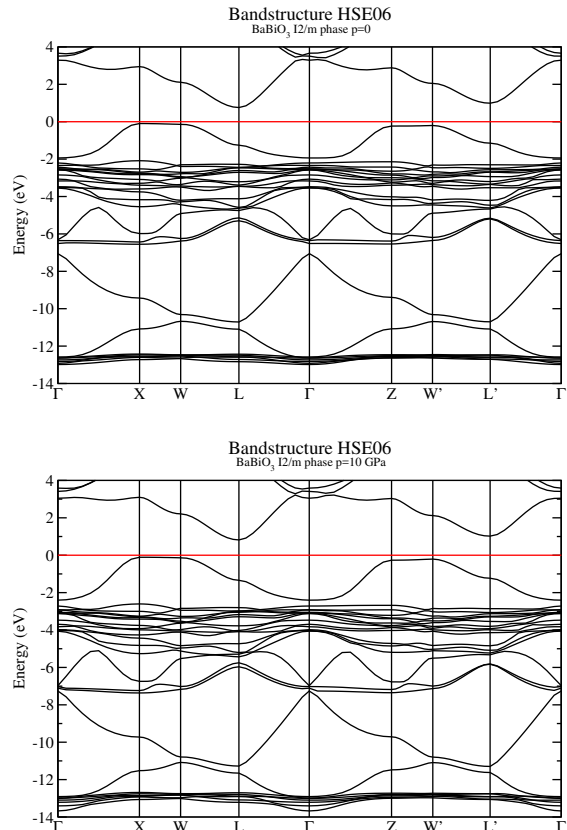


FIG. 8: HSE06 electronic structure of $I2/m$ BaBiO_3 at $P = 0$ and $P = 10$ GPa.

The pressure dependence obtained for HSE06 equilibrium electronic structures is shown for $I2/m$ at $P=0$ and 10 GPa in Fig.8 and for $P-1$ at $P=10$ and 20 GPa in Fig.9. The evolution is mild, and, as anticipated, there is no metallization under pressure. Despite the pressure-induced decrease of the relative bond disproportionation, there is in fact a slight increase of the electronic band gap, as shown in Fig.10. While that for $I2/m$ does not explain the data below 10 GPa the theoretical gap increase predicted for the $P-1$ phase agrees well with the observed resistivity increase between 10 and 40 GPa. Quantitatively, we predict a slope of about 52 meV/10 GPa which is rather satisfactory compared to experimental slope of 30 meV/10 GPa if one considers that even HSE06 functional is not designed to provide the exact value of the band gap. In summary, theory and experiment agree on BaBiO_3 becoming even more insulating upon pressure increase above 10 GPa. The experimental slight decrease of resistivity below 10 GPa could be caused by thermal

fluctuations affecting the rotation angle of the octahedra and in turn the band gap – temperature effects, here neglected, are expected to be more important precisely at low pressures.

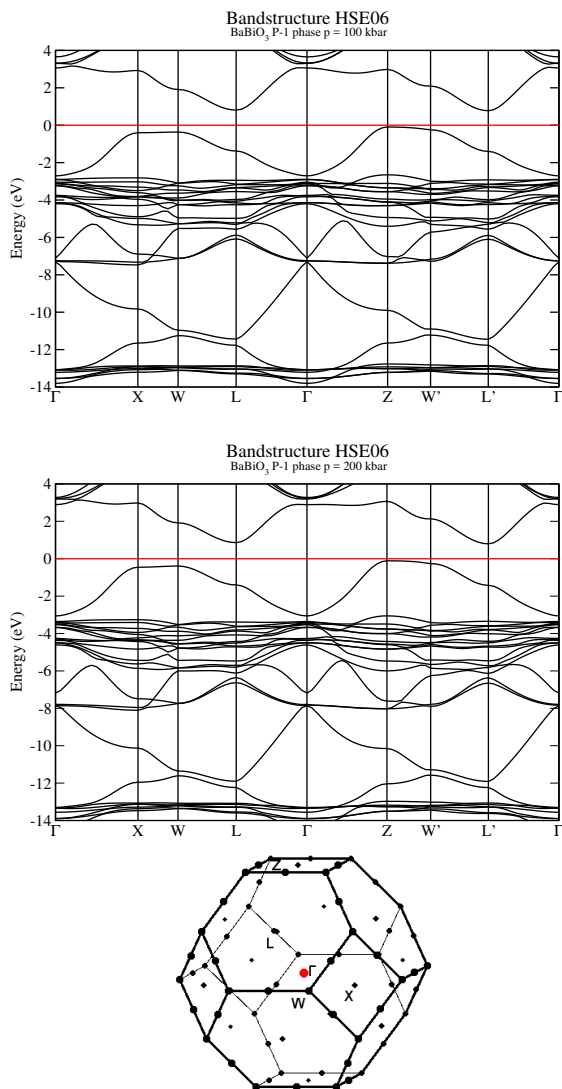


FIG. 9: HSE electronic structure of $P-1$ BaBiO_3 at $P=$ 10 and 20 GPa. On the bottom panel the Brillouin zone is shown.

The $C2/m$ phase at 40 and 50 GPa is semimetallic (valence and conduction band overlap by about 0.11 eV) – but as was said above the mixed-structure character of this phase suggests that it is probably small-cell artifact. Mixed structures arising for this reason are not uncommon in insulators, due to broken bonds at the interface. The $P1$ phase at 50 GPa has instead a large band gap of 2.95 eV and is a good insulator. If indeed the $C2/m$ phase is an artifact and $P-1$ survives even if metastable to 40-50 GPa, then at 50 GPa and beyond some disordered structures similar to insulating $P1$ might take over. The $P1$ gap at 40 GPa it is 3.01 eV so it increases upon decreasing pressure, which agrees with the slope of exper-

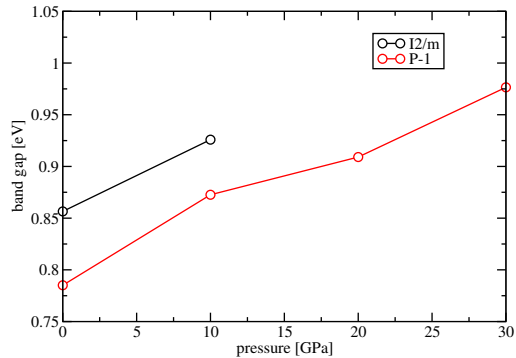


FIG. 10: Pressure dependence of HSE indirect band gap of BaBiO_3 in $I2/m$ and $P-1$ phases.

imental resistivity upon decompression down to 10 GPa where the disordered system might start recrystallizing.

V. DISCUSSION AND CONCLUSIONS

Our main result is that BaBiO_3 resists all tendencies towards equivalent $\text{Bi}(4+)$ ions under pressure. As pressure increases, structure changes so as to preserve two (or at least two) inequivalent valence states of the Bi ion, and either a frank insulating or a nearly insulating character along with that. This outcome may be seen as a surprise if the disproportionation of BaBiO_3 was interpreted as a Peierls-type CDW, suggesting that the persistent inequivalence of two Bi sites should be attributed to a different origin. One possible origin, which has been raised before, is an intrinsic intra-atomic tendency of the Bi ion to avoid valency $4+$, favoring either $3+$ or $5+$.

Further progress should be first of all experimental, identifying and confirming the high pressure phases, *in primis* our predicted pseudotetragonal $P-1$ phase (or the closely related tetragonal $I4/m$ phase) between 7 and 27 GPa and possibly beyond till 40 GPa by high-quality X-ray or neutron diffraction. Above 40 GPa, that search may be considerably complicated by the high levels of hysteresis which we found in resistivity, indicating that transitions to higher pressure structures might require a non-trivial rearrangement of atoms and reconstruction of structure. In closing, we can connect with a purely theoretical parallel study by another group¹³ where a similar sequence of phases has also been predicted, and which agrees with our overall conclusion of inequivalent Bi ions and (with the exception of $C2/m$, that does not show up in our experiments) that there is no metallic state in high-pressure BaBiO_3 .

Acknowledgments

This work was supported by the Slovak Research and Development Agency under Contract No. APVV-15-0496, by the VEGA project No. 1/0904/15 and by the project implementation 26220220004 within the Research & Development Operational Programme funded by the ERDF. Part of the calculations were performed in the Computing Centre of the Slovak Academy of Sci-

ences using the supercomputing infrastructure acquired in project ITMS 26230120002 and 26210120002 (Slovak infrastructure for high-performance computing) supported by the Research & Development Operational Programme funded by the ERDF. Work in Trieste was partly sponsored under ERC MODPHYSFRICT Contract 320796. We are grateful to Dr. Lilia Boeri for sharing with us the unpublished results of Ref.¹³.

-
- ¹ D.E.Cox and A.W.Sleight, Solid State Communications **19**, 969 (1976).
- ² T. M. Rice and L. Sneddon, Phys. Rev. Lett. **47**, 689 (1981), URL <https://link.aps.org/doi/10.1103/PhysRevLett.47.689>.
- ³ T. Thonhauser and K. M. Rabe, Phys. Rev. B **73**, 212106 (2006), URL <https://link.aps.org/doi/10.1103/PhysRevB.73.212106>.
- ⁴ R. J. Cava et al., Nature **332**, 814 (1988), URL <http://dx.doi.org/10.1038/332814a0>.
- ⁵ L. F. Mattheiss and D. R. Hamann, Phys. Rev. Lett. **60**, 2681 (1988), URL <https://link.aps.org/doi/10.1103/PhysRevLett.60.2681>.
- ⁶ B. J. Kennedy, C. J. Howard, K. S. Knight, Z. Zhang, and Q. Zhou, Acta Crystallographica **B62**, 537546 (2006).
- ⁷ A. W. Sleight, Physica C **514**, 152165 (2015).
- ⁸ L. F. Mattheiss and D. R. Hamann, Phys. Rev. B **28**, 4227 (1983), URL <https://link.aps.org/doi/10.1103/PhysRevB.28.4227>.
- ⁹ K. Kunc, R. Zeyher, A. Liechtenstein, M. Methfessel, and O. Andersen, Solid State Communications **80**, 325 (1991), ISSN 0038-1098, URL <http://www.sciencedirect.com/science/article/pii/003810989190139M>.
- ¹⁰ C. Franchini, A. Sanna, M. Marsman, and G. Kresse, Phys. Rev. B **81**, 085213 (2010), URL <https://link.aps.org/doi/10.1103/PhysRevB.81.085213>.
- ¹¹ D. Korotin, V. Kukolev, A. V. Kozhevnikov, D. Novoselov, and V. I. Anisimov, Journal of Physics: Condensed Matter **24**, 415603 (2012), URL <http://stacks.iop.org/0953-8984/24/i=41/a=415603>.
- ¹² D. Ceresoli and E. Tosatti, unpublished.
- ¹³ A. Smolyanyuk, L. Boeri, and C. Franchini, ArXiv e-prints (2017), 1702.04600.
- ¹⁴ Z. Akhtar, M. Akhtar, S. Clark, and C. Catlow, Solid State Communications **92**, 535 (1994), ISSN 0038-1098, URL <http://www.sciencedirect.com/science/article/pii/0038109894904936>.
- ¹⁵ H. Sugiura and T. Yamadaya, Physica **139 & 140B**, 349 (1986).
- ¹⁶ L. X. Jun and M. Yutaka, Chinese Phys. Lett. **20**, 2027 (2003).
- ¹⁷ Y. Imai, M. Kato, T. Noji, Y. Koike, M. Hedo, Y. Uwatoko, and N. Mori, Physica C **426431**, 497499 (2005).
- ¹⁸ A. Oganov and C. Glass, J. Chem. Phys. **124**, 244704 (2006).
- ¹⁹ A. Laio and M. Parrinello, Proc. Natl. Acad. Sci. USA **99**, 12562 (2002).
- ²⁰ R. Martoňák, A. Laio, and M. Parrinello, Phys. Rev. Lett. **90**, 075503 (2003).
- ²¹ R. Martoňák, D. Donadio, A. R. Oganov, and M. Parrinello, Nature Materials **5**, 623 (2006).
- ²² D. C. Lonie and E. Zurek, Computer Physics Communications **182**, 372 (2011).
- ²³ G. Kresse and J. Furthmüller, Phys. Rev. B **54**, 11169 (1996).
- ²⁴ G. Kresse and D. Joubert, Phys. Rev. B **59**, 1758 (1999).
- ²⁵ J. P. Perdew, K. Burke, and M. Ernzerhof, Phys. Rev. Lett. **77**, 3865–3868 (1996).
- ²⁶ H. J. Monkhorst and J. D. Pack, Phys. Rev. B **13**, 5188 (1976).
- ²⁷ A. V. Krukau, O. A. Vydrov, A. F. Izmaylov, and G. E. Scuseria, The Journal of Chemical Physics **125**, 224106 (pages 5) (2006).
- ²⁸ J. Heyd, G. E. Scuseria, and M. Ernzerhof, The Journal of Chemical Physics **124**, 219906 (2006).
- ²⁹ H. Unoki and T. Sakudo, J. Phys. Soc. Jpn. **23**, 546 (1967).
- ³⁰ M. Parrinello and A. Rahman, Phys. Rev. Lett. **45**, 1196 (1980).
- ³¹ Cif files with structural data of the new structures are in Supplementary material.